Chapter 1
PET Radiotracers for Tumor Imaging

Ming-Rong Zhang

1.1 Introduction

Positron emission tomography (PET) is a nuclear medicine imaging technique that produces a three-dimensional functional image of the living body. This system detects pairs of gamma rays emitted indirectly by a positron-emitting radiotracer, which is introduced into the body as a biologically active tracer. Three-dimensional images of radiotracer concentration within the body are then constructed by computer graphic analysis. PET is both a medical and study tool used in clinical oncology (medical imaging and diagnosis of tumors and the search for metastases) and in preclinical animal studies, where it allows repeated scans of the same subject. PET is particularly valuable in cancer research because it increases the statistical quality of the data (research subjects can act as their own controls) and substantially reduces the number of animals needed for individual studies.

PET studies using radiotracers are leading to rapid advances in the personalized diagnosis and treatment of cancers. The ability to translate oncogene signatures into functional imaging data, such as those obtained using PET via specific targeted radiotracers, permits noninvasive and quantitative visualization of tumors at multiple time points and at the whole-body level, thereby facilitating personalized drug development, clinical trials, and patient management.

The development of labeled radiotracers using positron-emitting radionuclides is required for the PET technique. In this review, the author will introduce [^{18}F]FDG and post-[^{18}F]FDG radiotracers, review recent advances in the development of PET tumor imaging radiotracers, and present results to develop novel PET radiotracers for tumor imaging.

M.-R. Zhang (✉)
Department of Radiopharmaceutics Development, National Institute of Radiological Sciences, National Institutes for Quantum and Radiological Science and Technology, 4-9-1 Anagawa, 263-8555 Inage-ku, Chiba, Japan
e-mail: zhang@nirs.go.jp

© Springer Nature Singapore Pte Ltd. 2017

T. Inoue et al. (eds.), *Personalized Pathway-Activated Systems Imaging in Oncology*, DOI 10.1007/978-981-10-3349-0_1

1.2 [^{18}F]FDG for Glucose Metabolism

PET scanning with the radiotracer [^{18}F]FDG (Fig. 1.1) is widely used in tumor imaging for clinical studies or diagnosis [1–3]. This radiotracer is derived from glucose, taken up by glucose-consuming cells and phosphorylated by mitochondrial hexokinase, which is greatly elevated in rapidly growing malignant tumors. Because the hydroxyl group in glucose (replaced by ^{18}F to generate [^{18}F]FDG) is required for the next step in the glucose metabolism in all cells, [^{18}F]FDG cannot participate in further reactions [4]. Furthermore, most tissues, except the liver and kidneys, cannot remove the phosphate added by the hexokinase. This means that [^{18}F]FDG is trapped in cells that take it up until it decays, owing to their ionic properties and phosphorylated sugars, which cannot be cleared from cells. This results in high level of radioactivity accumulating in tissues with high glucose uptake and metabolism, such as the brain, liver, and most cancers [5–10]. As a result, [^{18}F]FDG-PET can be used for cancer diagnosis, staging, and monitoring of therapy [11]. Many individual solid tumors have been found to exhibit very high uptake of radioactivity, a fact that is useful when searching for tumor metastasis or for recurrence after the removal of a primary tumor known to be highly active. PET oncology scans using [^{18}F]FDG make up over 90 % of all PET scans in the current medical practice.

Although PET facilities are rapidly increasing worldwide, the only PET radiopharmaceutical currently available for diagnosis is [^{18}F]FDG. In keeping with this notion, [^{18}F]FDG is by far the most widely used radiotracer for clinical purposes, but its application has some shortcomings. Since [^{18}F]FDG is a derivative of glucose, which is taken up by cells via glucose transporters, phosphorylated by hexokinase, and retained in the tissue, its high uptake is not only in tumor cells but also in normal tissues, such as the brain and heart, which have high levels of glucose metabolic activity [12, 13]. Hence, [^{18}F]FDG-PET is not suitable for imaging tumors in these tissues. In addition, because of its high uptake in urine and fast excretion from the bladder, it is difficult to detect tumors in this organ and surrounding tissues using [^{18}F]FDG [5]. Most importantly, because of high uptake in inflamed tissues, it is difficult to distinguish tumor from inflammation using [^{18}F]FDG.

To increase the usefulness of PET and to overcome the disadvantages associated with [^{18}F]FDG, it is important to develop new imaging radiotracers, which use alternative mechanisms for tumor visualization and provide different information to that obtained using [^{18}F]FDG. Moreover, higher tumor specificity than the one provided by [^{18}F]FDG could be achieved using new radiotracers.

In the following sections, the author will introduce the main candidates for post-[^{18}F]FDG tumor imaging radiotracers.

Fig. 1.1 [^{18}F]FDG

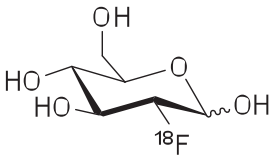

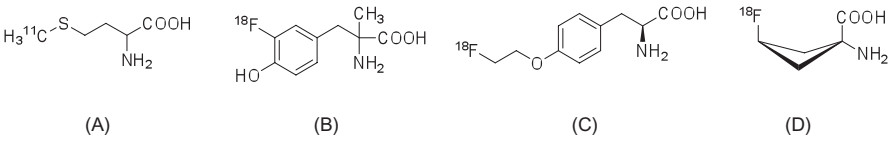

(A) (B) (C) (D)

Fig. 1.2 (**a**) [^{11}C]Met, (**b**) [^{18}F]FMT, (**c**) [^{18}F]FET, and (**d**) [^{18}F]FACBC

1.3 Amino Acids

The amino acid analog most frequently used as a radiotracer is [^{11}C]methionine ([^{11}C]Met, Fig. 1.2) [14, 15]. [^{11}C]Met is easily synthesized using [^{11}C]methyl iodide or [^{11}C]methyl triflate as the radiolabeling agent. Since the precursor for [^{11}C]Met radiosynthesis is L-homocysteine, the product obtained is only the L-isomer. In the normal brain, where protein metabolism levels are low, PET radiotracers reflecting controlled protein biosynthesis/degradation rates are suitable for the detection of glioma tumors in many PET facilities [16, 17]. However, because the S-[^{11}C]methyl group in the cell is relatively easily transferred into other positions, compared to ^{11}C labeling in other positions, the levels of [^{11}C]Met are insufficient to enable evaluation of protein synthesis ability.

Since 1960, amino acids that are stable against metabolism (unlike natural amino acids) have been developed. These artificial amino acids were labeled with ^{11}C and used to detect tumors in preclinical studies. Among them, α-aminoisobutanoic acid, α-aminocyclobutane-1-carboxylic acid, and α-aminocyclopentane-1-carboxylic acid show high binding affinity for amino acid transporters. Moreover, these amino acid analogs do not contain chiral carbon atoms; therefore, their radiolabeled versions are considered promising probes for tumor imaging.

Many ^{18}F-labeled amino acid analogs have been developed and evaluated as candidate of post-[^{18}F]FDG radiotracers (Fig. 1.2). Although phenylalanine and tyrosine analogs were found to correlate with protein synthesis, these analogs are unable to participate in protein synthesis, and their tumor uptake levels are associated with amino acid transporter activity. Then, in efforts to improve in vivo metabolic stability, 3-[^{18}F]fluoro-α-methyl-L-tyrosine ([^{18}F]FMT, Fig. 1.2) [18] and 4-[^{18}F]fluoroethyl-L-tyrosine ([^{18}F]FET) [19] were developed. More recently, [^{18}F]FACBC has been reported as the most promising radiolabeled amino acid analog [20, 21]. This radiotracer has two stereoisomers, with the cis isomer exhibiting higher selectivity than the anti-isomer. In clinical glioblastoma imaging studies, which cannot use [^{18}F]FDG-PET, [^{18}F]FACBC can provide high-quality PET tumor images.

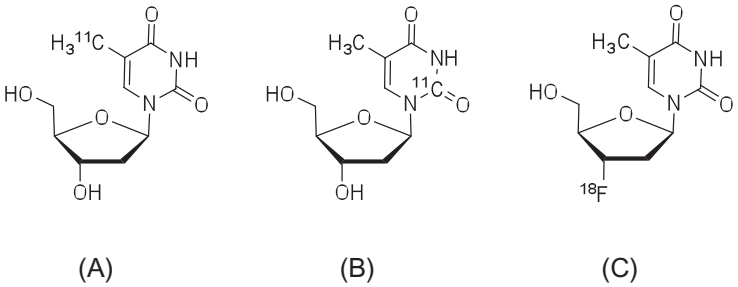

Fig. 1.3 (**a**) [^{11}C]Methylthymidine, (**b**) 2-[^{11}C]thymidine, and (**c**) [^{18}F]FLT

Therefore, the ^{18}F-labeled artificial amino acid analogs are viable alternatives for the detection of tumors that cannot be successfully visualized by [^{18}F]FDG-PET.

1.4 Nucleic Acids

[^{3}H]Methylthymidine has been synthesized and used for many years. In addition, methods for production and in vivo evaluation of the PET tracers [^{11}C]methylthymidine (Fig. 1.3) and 2-[^{11}C]thymidine have been reported since 1980 [22, 23]. However, these natural nucleic acid analogs are not stable in vivo, which prompted the modification of their chemical structures and radiolabeling them with ^{18}F, thus creating a probe a longer half-life than ^{11}C.

3′-Deoxy-3′-[^{18}F]fluorothymidine ([^{18}F]FLT) is an analog of thymidine, in which ^{18}F is introduced in the 3′-position and shows high in vivo stability and strong resistance to metabolism by cellular thymidine phosphatase [24]. Blood circulating [^{18}F]FLT is taken up by the tissues via a pyrimidine transporter, which functions in nucleic acid synthesis. As the hydroxyl group in 3′-position is replaced by fluorine, phosphorylated [^{18}F]FLT-5′-P cannot participate in the synthesis of DNA, and it is thus retained in the cell as a monophosphate. Hence, the uptake of [^{18}F]FLT can reflect thymidine kinase-1 (TK1) activity in tumor cells [25], which is very low in the G0 stage of the cell cycle and reaches a maximum between the G1 and S phases. Therefore, [^{18}F]FLT has been used to evaluate cell proliferation for tumor staging and assess the therapeutic effects of anticancer drugs.

1.5 Lipid Metabolism

Cancer is characterized by the high proliferation ability of tumor cells, and during this process the synthesis of cell membrane components increases accordingly. Therefore, membrane lipid synthesis is a useful target to also evaluate the

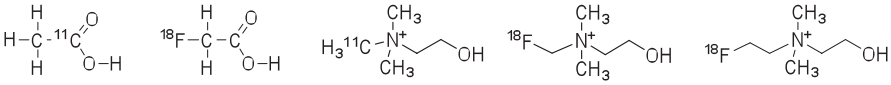

Fig. 1.4 (**a**) [^{11}C]Acetate, (**b**) [^{18}F]fluoroacetate, (**c**) [^{11}C]choline, (**d**) [^{18}F]fluoromethylcholine, and (**e**) [^{18}F]fluoroethylcholine

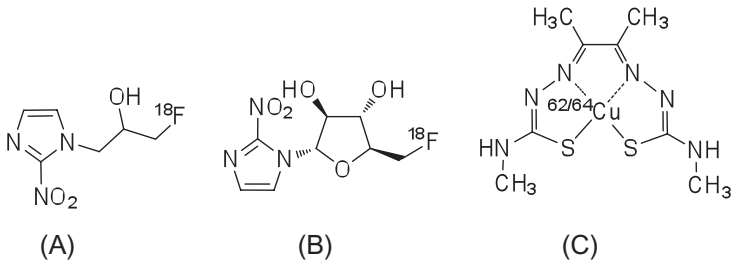

Fig. 1.5 (**a**) [^{18}F]FMISO, (**b**) [^{18}F]FAZA, and (**c**) $^{62/64}$Cu-ATSM

proliferation ability of tumor cells. To this end, [^{11}C]acetate, [^{11}C]choline, and [^{18}F] fluorocholine have been developed and used in clinical imaging studies (Fig. 1.4) [26].

In vitro evaluation of [^{11}C]acetate has been performed to determine the mechanism of radioactivity accumulation in tumor cells [27]. Acetate is formed by the metabolism of phosphatidylcholine and neutral lipids, and, thus, the accumulation of [^{11}C]acetate radioactivity can reflect the proliferation ability of tumor cells [28, 29].

The uptake of choline analogs can reflect the activity of choline kinase and be used to indirectly evaluate ability to synthesize membrane lipids [30–32]. In clinical studies, PET radiotracers for lipid metabolism are useful for the detection of tumors in the brain, the bladder, and the urinary tract. [^{11}C/^{18}F]Choline analogs are not useful for the detection of cancer in epigastrium tissues and other organs because they have a high radioactivity uptake in the liver. Hence, acetate- and choline-based radiotracers may be better to evaluate the therapeutic effects of radiation and antitumor drugs.

1.6 Hypoxia

During the process of tumor cell proliferation, insufficient supply of oxygen results in hypoxia. Hypoxic areas of tumors are relatively insensitive to chemotherapy and radiation therapy. Thus, an understanding of the hypoxic state is useful for the prediction of therapeutic effects and the evaluation of treatment regimens, which has led to the development of PET imaging radiotracers designed to evaluate hypoxia

[33–35]. [^{18}F]FMISO (Fig. 1.5) was the first nitroimidazole analog used for imaging of hypoxia in tumors [33]. The nitro group of misonidazole analogs is reduced to form a hydrophilic amine group, and this amine product binds to cellular components and is retained in tumor cells.

In hypoxic areas, which have a low blood flow, the initial uptake of radioactivity by one-pass circulation of radiotracer is low. However, the highly lipophilic [^{18}F]FMISO is able to diffuse into the regions with low blood flow. Unfortunately, the slow clearance of radioactivity from blood means that PET imaging with [^{18}F]FMISO may not result in high-quality images, and thus, extended scanning durations are required [36]. As an alternative, the tracer [^{18}F]FAZA, which has low lipophilicity and high hydrophilicity, has been developed and used in clinical studies [37, 38]. Compared to [^{18}F]FMISO, [^{18}F]FAZA shows improved solubility in water and good signal/noise contrast in PET images within a relatively short PET scanning time.

In addition to nitroimidazole analogs, $^{62/64}$Cu-diacetyl-bis(N-4-methylthiosemicarbazone ($^{62/64}$Cu-ATSM) is also a useful PET imaging radiotracer for hypoxia [39, 40]. Cu-ATSM is a small lipophilic molecular complex that easily penetrates the blood-brain barrier and cellular membranes and clears rapidly from normal tissues [41]. In hypoxic area, Cu^{2+} binding to ATSM is reduced to Cu^{+} by microsomal electron transfer, and the Cu^{+} component is retained in the cell. Compared to [^{18}F]FMISO, $^{62/64}$Cu-ATSM shows rapid clearance from normal tissues and blood to produce images with good contrast and signal/noise ratios within a short PET scanning time.

1.7 Receptor and Angiogenesis

By transferring signals through various receptors overexpressed in tumor cells, certain genes and proteins mediate tumor phenotypes, including proliferation ability, invasiveness, metastasis, and treatment resistance. PET studies using radiolabeled tracers for imaging of these receptors are useful for understanding the tumor characteristics.

To date, a large number of PET radiotracers for imaging of receptors have been reported. Major radiotracers of this type include: epidermal growth factor receptor (EGFR) human type (HER2), which is associated with poor prognosis in breast cancer; folic acid receptor, associated with malignant proliferation; chemokine receptor, associated with metastasis; glucagon-like peptide-1 (GLP-1) receptor, associated with neuroendocrine tumors; somatostatin receptor; tumor angiogenesis integrin receptor ($\alpha v\beta 3$); and vascular endothelial growth factor (VEGF) [42]. A number of these radiotracers have been used in clinical studies.

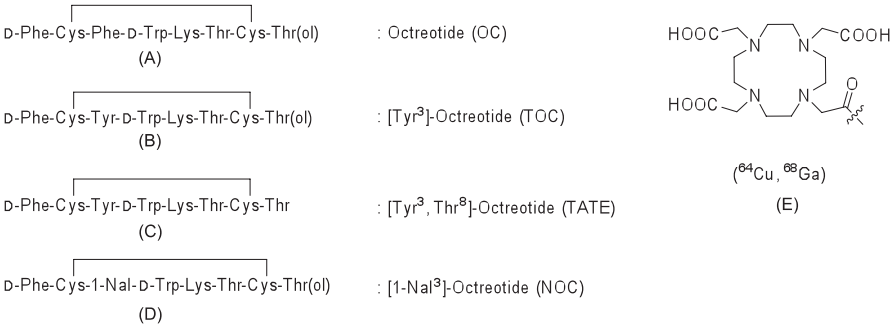

Fig. 1.6 PET radiotracers targeting somatostatin receptors: (**a**) octreotide, (**b**) [Tyr^3]-octreotide, (**c**) [Tyr^3,Thr^8]-octreotide, (**d**) [1-Nal^3]-octreotide, and (**e**) NOC-conjugated 1,4,7,10-tetraazacyclododecane

1.7.1 Somatostatin Receptors

Somatostatin receptors are G protein-coupled transmembrane proteins that are widely distributed in normal tissues, including those of the central nervous system, pancreas, anterior pituitary, thyroid gland, spleen, gastrointestinal tract, and adrenal gland. There are five somatostatin receptors, of which somatostatin receptor-2 is overexpressed in the majority of malignant tumors, including neuroendocrine cancers, small cell lung cancer, breast cancer, and malignant lymphoma. The endogenous ligand of somatostatin receptors, somatostatin, has two isoforms of 14 and 28 amino acids, both of which demonstrate high binding affinity for somatostatin receptors. Owing to its short half-life in blood (2 min), imaging using somatostatin as a radiotracer is difficult. An analog of somatostatin, octreotide, which is formed from eight amino acid residues, has a longer half-life in blood (1.7 h) and higher metabolic stability than somatostatin. Many PET radiotracers derived from octreotide have been developed. Their chemical structures are illustrated in Fig. 1.6.

The PET radiotracers for somatostatin receptors, TOC, TATE, NOC-conjugated1,4,7,10-tetraazacyclododecane (DOTA), ^{68}Ga-DOTATOC, ^{68}Ga-DOTATATE, and ^{68}Ga-DOTANOC] have been used in clinical studies (Fig. 1.6) [43, 44].

1.7.2 Integrin Receptor Subtype αvβ3

Angiogenesis is an important process during the proliferation of solid tumors. Cilengitide is a treatment developed to target integrin receptor (subtypes αvβ3 and αvβ5), which attenuates tumor angiogenesis. Almost all PET radiotracers targeting integrins contain the amino acid sequence, arginine-glycine-asparagine (RGD) [45, 46]. The RGD sequence, which is commonly found in extracellular matrix proteins,

binds to integrins and shows particularly high affinity for the integrin αv subunit. Representative integrin-targeting PET radiotracers are ^{18}F-, ^{68}Ga-, and ^{64}Cu-labeled compounds, including [^{18}F]galacto-RGD, [^{18}F]fluciclatide (AH111585), [^{18}F]RGD-K5, ^{64}Cu-DOTA-RGD, and ^{68}Ga-NOTA-RGD (Fig. 1.7).

1.7.3 Other Receptors Involved in Tumor Angiogenesis

Another promising target molecule involved in tumor angiogenesis is VEGF. VEGF and its receptor VEGFR are highly expressed in endothelial cells, and VEGFR is a promising target for PET imaging [47]. To that end the VEGFR tyrosine kinase inhibitor sunitinib and VEGF monoclonal antibody bevacizumab were developed to image this pathway. Recently, bevacizumab and ranibizumab have been labeled using ^{89}Zr (half-life, 78 h). ^{89}Zr-bevacizumab and ^{89}Zr-ranibizumab have demonstrated promise as potential PET imaging radiotracers for in vivo imaging of VEGF in tumor-bearing mice [48, 49].

PET imaging studies using octreotide-based and RGD-peptide-based molecules to target somatostatin and integrin receptors, respectively, have had some success in clinical studies. The imaging data resulting from targeting these molecules may be useful in clinical diagnosis, tumor staging, therapeutic strategies, and monitoring therapeutic effects. However, the clinical importance of imaging somatostatin and integrin receptors has not yet been fully determined, and more research is required to validate their clinical usefulness.

1.8 Metabotropic Glutamate 1 Receptor

Ectopic metabotropic glutamate 1 receptor (mGluR1) shows oncogenic activity and is becoming an important target for personalized diagnosis and treatment strategies for melanomas [50]. Evidence indicates that ectopically expressed mGluR1 independently induces melanocyte carcinogenesis. We have developed an oncoprotein-based PET imaging platform in melanomas for noninvasive visualization and quantitation of mGluR1 with a novel mGluR1-specific radiotracer, 4-[^{18}F]fluoro-*N*-[4-[6-(isopropylamino)pyrimidin-4-yl]-1,3-thiazol-2-yl]-*N*-methylbenzamide ([^{18}F]FITM; Fig. 1.8) [50]. [^{18}F]FITM shows excellent pharmacokinetics, namely, the dense and specific accumulation of radioactivity in mGluR1-positive melanomas B16F1 and B16F10, compared to mGluR1-negative hepatoma and normal tissues. Furthermore, accumulation levels of radioactivity corresponded to the extent of the tumor and to those of mGluR1 protein expression in melanomas and melanoma metastases in the lung (Fig. 1.8). The [^{18}F]FITM PET imaging platform is expected to open a new avenue for defining individualized therapeutic strategies, clinical trials, and patient management, as a noninvasive personalized diagnostic

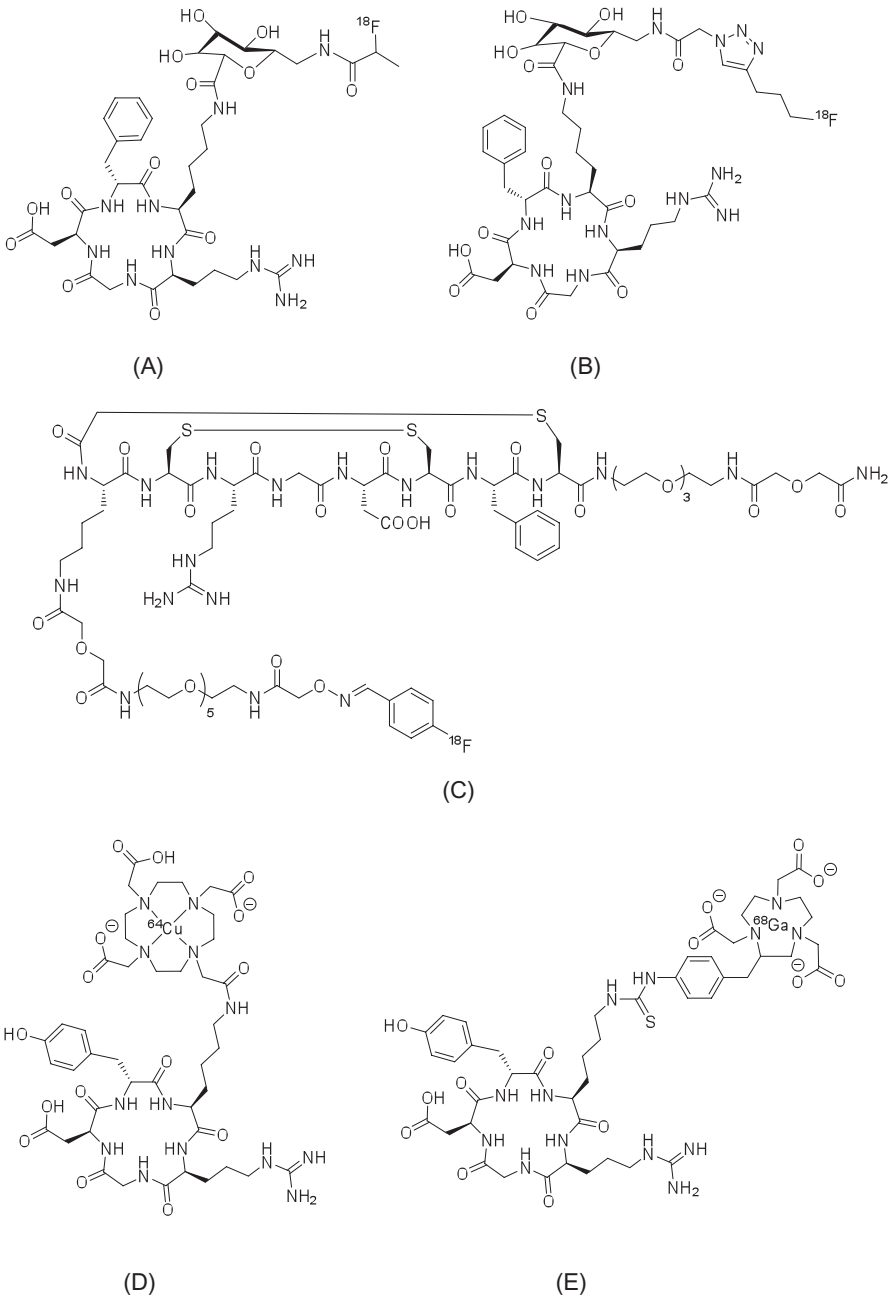

Fig. 1.7 (**a**) [^{18}F]Galacto-RGD, (**b**) [^{18}F]fluciclatide, (**c**) [^{18}F]RGD-K5, (**d**) ^{64}Cu-DOTA-RGD, and (**e**) ^{68}Ga-NOTA-RGD

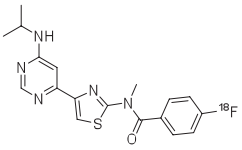

(A) [18F] FITM

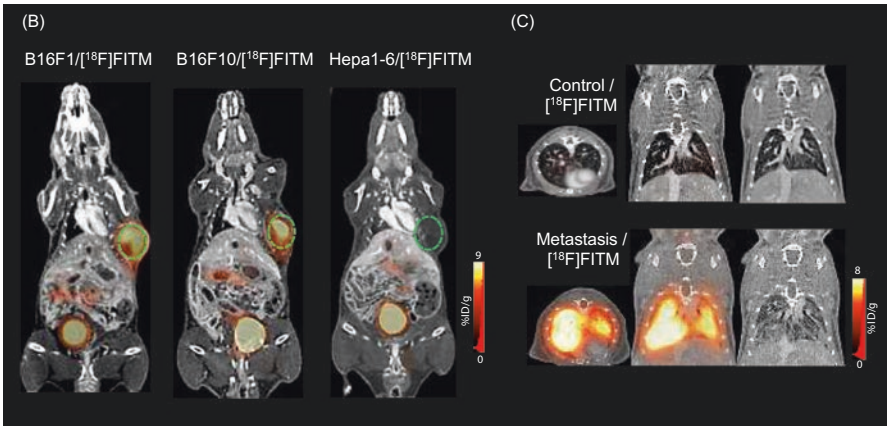

Fig. 1.8 (**a**) Chemical structure of [^{18}F]FITM. (**b**) Representative coronal [^{18}F]FITM PET/CT images in B16F1-, B16F10-, and Hepa1-6 tumor-bearing mice. High accumulation of radioactivity was observed in the mGluR1-positive B16F1 and B16F10 melanomas, and low uptake was observed in the mGluR1-negative Hepa1-6 tumor. *Green circles* indicate tumors. (**c**) Representative coronal and axial [^{18}F]FITM PET/CT images in mice with pulmonary metastatic melanoma and control mice without metastasis. Intense and heterogeneous accumulation of radioactivity was observed in the lungs bearing B16F10 metastasis with very low background signals

tool. It can also become a useful research means to understand mGluR1-triggered oncologic events in melanomas. Recently, an iodine analog of [^{18}F]FITM has been developed, and this compound can be further developed using ^{124}I and ^{131}I radiolabeling for long-duration PET scanning and radiotherapeutic applications [51].

1.9 Summary

Many PET radiotracers have been developed for imaging tumors to facilitate animal studies, clinical diagnosis, tumor staging, therapeutic strategy, and monitoring therapeutic effects. However, PET radiotracers for imaging a large number of molecular targets remain undeveloped. Moreover, as the targeted candidate molecules include small molecule compounds, peptides, and antibodies, determining how to label them efficiently using positron-emitted radionuclides is a challenging problem for their development as novel PET radiotracers. Radiolabeling techniques, including radionuclide production, preparation of radiolabeling agents, radiochemical

reactions, and automated production, continue to be assessed. Clearly, it will take a great deal of time and effort to identify another gold standard PET radiotracer for tumor imaging that is similar or more specific than [^{18}F]FDG.

Acknowledgment The author thanks Dr. Masayuki Fujinaga (National Institute of Radiological Sciences) for assistance in the preparation of this manuscript.

References

1. Ido T, Wan C-N, Fowler JS, et al. Labeled 2-deoxy-D-glucose analogs, 18F-labeled 2-deoxy-2-fluoro-D-glucose, 2-deoxy-2-fluoro-D-mannose and 14C-2-deoxy-2-fluoro-glucose. J Label Compd Radiopharm. 1978;14:171–83.
2. Reivich M, Kuhl D, Wolf A, et al. The [18F]fluorodeoxyglucose method for the measurement of local cerebral glucose utilization in man. Circ Res. 1979;44:127–37.
3. Yonekura Y, Benua RS, Brill AB, et al. Increased accumulation of 2-deoxy-2-[18F]Fluoro-D-glucose in liver metastases from colon carcinoma. J Nucl Med. 1982;23(12):1133–7.
4. Buck AK, Schirrmeister H, Mattfeldt T, et al. Biological characterisation of breast cancer by means of PET. Eur J Nucl Med Mol Imaging Suppl. 2004;1:S80–7.
5. Delbeke D. Oncological applications of FDG PET imaging. J Nucl Med. 1999;40(10):1706–15.
6. Buck AK, Schirrmeister H, Mattfeldt T, et al. Biological characterisation of breast cancer by means of PET. Eur J Nucl Med Mol Imaging. 2004;31(Suppl 1):S80–7.
7. Gambhir SS, Czernin J, Schwimmer J, et al. A tabulated summary of the FDG PET literature. J Nucl Med. 2001;42(5 Suppl):1S–93S.
8. Higashi T, Tamaki N, Torizuka T, et al. FDG uptake, GLUT-1 glucose transporter and cellularity in human pancreatic tumors. J Nucl Med. 1998;39(10):1727–35.
9. Higashi T, Saga T, Nakamoto Y, et al. Relationship between retention index in dual-phase (18) F-FDG PET, and hexokinase-II and glucose transporter-1 expression in pancreatic cancer. J Nucl Med. 2002;43(2):173–80.
10. De Gaetano AM, Rufini V, Castaldi P, et al. Clinical applications of (18)F-FDG PET in the management of hepatobiliary and pancreatic tumors. Abdom Imaging. 2012;37(6):983–1003.
11. Weber WA. Use of PET for monitoring cancer therapy and for predicting outcome. J Nucl Med. 2005;46(6):983–95.
12. Bleeker-Rovers CP, Vos FJ, Corstens FH, et al. Imaging of infectious diseases using [18F] fluorodeoxyglucose PET. Q J Nucl Med Mol Imaging. 2008;52(1):17–29.
13. Tarkin JM, Joshi FR, Rudd JH. PET imaging of inflammation in atherosclerosis. Nat Rev Cardiol. 2014;11(8):443–57.
14. Glaudemans AW, Enting RH, Heesters MA, et al. Value of 11C-methionine PET in imaging brain tumours and metastases. Eur J Nucl Med Mol Imaging. 2013;40(4):615–35.
15. Jager PL, Vaalburg W, Pruim J, et al. Radiolabeled amino acids: basic aspects and clinical applications in oncology. J Nucl Med. 2001;42(3):432–45.
16. Crippa F, Alessi A, Serafini GL. PET with radiolabeled amino acid. Q J Nucl Med Mol Imaging. 2012;56(2):151–62.
17. Gulyás B, Halldin C. New PET radiopharmaceuticals beyond FDG for brain tumor imaging. Q J Nucl Med Mol Imaging. 2012;56(2):173–90.
18. Inoue T, Shibasaki T, Oriuchi N, et al. 18F alpha-methyl tyrosine PET studies in patients with brain tumors. J Nucl Med. 1999;40(3):399–405.
19. Wester HJ, Herz M, Weber W, et al. Synthesis and radiopharmacology of O-(2-[18F] fluoroethyl)-L-tyrosine for tumor imaging. J Nucl Med. 1999;40(1):205–12.

20. Shoup TM, Olson J, Hoffman JM, et al. Synthesis and evaluation of [18F]1-amino-3-fluorocyclobutane-1-carboxylic acid to image brain tumors. J Nucl Med. 1999;40(2):331–8.
21. Schuster DM, Nanni C, Fanti S, et al. Anti-1-amino-3-18F-fluorocyclobutane-1-carboxylic acid: physiologic uptake patterns, incidental findings, and variants that may simulate disease. J Nucl Med. 2014;55(12):1986–92.
22. Martiat P, Ferrant A, Labar D, et al. In vivo measurement of carbon-11 thymidine uptake in non-Hodgkin's lymphoma using positron emission tomography. J Nucl Med. 1988;29(10):1633–7.
23. Tehrani OS, Shields AF. PET imaging of proliferation with pyrimidines. J Nucl Med. 2013;54(6):903–12.
24. Wagner M, Seitz U, Buck A, et al. 3'-[18F]fluoro-3'-deoxythymidine ([18F]-FLT) as positron emission tomography tracer for imaging proliferation in a murine B-Cell lymphoma model and in the human disease. Cancer Res. 2003;63(10):2681–7.
25. Chalkidou A, Landau DB, Odell EW, et al. Correlation between Ki-67 immunohistochemistry and 18F-fluorothymidine uptake in patients with cancer: a systematic review and meta-analysis. Eur J Cancer. 2012;48(18):3499–513.
26. Brogsitter C, Zöphel K, Kotzerke J. 18F-Choline, 11C-choline and 11C-acetate PET/CT: comparative analysis for imaging prostate cancer patients. Eur J Nucl Med Mol Imaging. 2013;40(Suppl 1):S18–27.
27. Yoshimoto M, Waki A, Yonekura Y, et al. Characterization of acetate metabolism in tumor cells in relation to cell proliferation: acetate metabolism in tumor cells. Nucl Med Biol. 2001;28(2):117–22.
28. Deford-Watts LM, Mintz A, Kridel SJ. The potential of ^{11}C-acetate PET for monitoring the Fatty acid synthesis pathway in Tumors. Curr Pharm Biotechnol. 2013;14(3):300–12.
29. Liu D, Khong PL, Gao Y. Radiation dosimetry of whole-body dual tracer 18F-FDG and 11C-acetate PET/CT for hepatocellular carcinoma. J Nucl Med. 2016;57(6):907. pii: jnumed.115.165944.
30. Hara T, Kosaka N, Kishi H. PET imaging of prostate cancer using carbon-11-choline. J Nucl Med. 1998;39(6):990–5.
31. Hara T. 18F-fluorocholine: a new oncologic PET tracer. J Nucl Med. 2001;42(12):1815–7.
32. Hara T, Kosaka N, Kishi H. Development of (18)F-fluoroethylcholine for cancer imaging with PET: synthesis, biochemistry, and prostate cancer imaging. J Nucl Med. 2002;43(2):187–99.
33. Valk PE, Mathis CA, Prados MD, et al. Hypoxia in human gliomas: demonstration by PET with fluorine-18-fluoromisonidazole. J Nucl Med. 1992;33(12):2133–7.
34. Lewis JS, Welch MJ. PET imaging of hypoxia. Q J Nucl Med. 2001;45(2):183–8.
35. Fleming IN, Manavaki R, Blower PJ, et al. Imaging tumour hypoxia with positron emission tomography. Br J Cancer. 2015;112(2):238–50.
36. Peeters SG, Zegers CM, Yaromina A, et al. Current preclinical and clinical applications of hypoxia PET imaging using 2-nitroimidazoles. Q J Nucl Med Mol Imaging. 2015;59(1):39–57.
37. Postema EJ, McEwan AJ, Riauka TA, et al. Initial results of hypoxia imaging using 1-alpha-D: -(5-deoxy-5-[18F]-fluoroarabinofuranosyl)-2-nitroimidazole (18F-FAZA). Eur J Nucl Med Mol Imaging. 2009;36(10):1565–73.
38. Saga T, Inubushi M, Koizumi M, et al. Prognostic value of PET/CT with 18F-fluoroazomycin arabinoside for patients with head and neck squamous cell carcinomas receiving chemoradiotherapy. Ann Nucl Med. 2016;30(3):217–24.
39. Fujibayashi Y, Taniuchi H, Yonekura Y, et al. Copper-62-ATSM: a new hypoxia imaging agent with high membrane permeability and low redox potential. J Nucl Med. 1997;38(7):1155–60.
40. Lewis J, Laforest R, Buettner T, et al. Copper-64-diacetyl-bis(N4-methylthiosemicarbazone): an agent for radiotherapy. Proc Natl Acad Sci U S A. 2001;98(3):1206–11.
41. Furukawa T, Yuan Q, Jin ZH, et al. Comparison of intratumoral FDG and Cu-ATSM distributions in cancer tissue originated spheroid (CTOS) xenografts, a tumor model retaining the original tumor properties. Nucl Med Biol. 2014;41(8):653–9.

42. Ambrosini V, Fani M, Fanti S, et al. Radiopeptide imaging and therapy in Europe. J Nucl Med. 2011;52(Suppl 2):42S–55S.
43. Ambrosini V, Campana D, Polverari G, et al. Prognostic value of 68Ga-DOTANOC PET/CT SUVmax in patients with neuroendocrine tumors of the pancreas. J Nucl Med. 2015;56(12):1843–8.
44. Lu X, Wang RF. A concise review of current radiopharmaceuticals in tumor angiogenesis imaging. Curr Pharm Des. 2012;18(8):1032–40.
45. Johnbeck CB, Knigge U, Kjær A. PET tracers for somatostatin receptor imaging of neuroendocrine tumors: current status and review of the literature. Future Oncol. 2014;10(14):2259–77.
46. Chen H, Niu G, Wu H, et al. Clinical application of radiolabeled RGD peptides for PET imaging of integrin αvβ3. Theranostics. 2016;6(1):78–92.
47. Jubb AM, Harris AL. Biomarkers to predict the clinical efficacy of bevacizumab in cancer. Lancet Oncol. 2010;11(12):1172–83.
48. van der Bilt AR, Terwisscha van Scheltinga AG, Timmer-Bosscha H, et al. Measurement of tumor VEGF-A levels with 89Zr-bevacizumab PET as an early biomarker for the antiangiogenic effect of everolimus treatment in an ovarian cancer xenograft model. Clin Cancer Res. 2012;18(22):6306–14.
49. Nagengast WB, Lub-de Hooge MN, Oosting SF, et al. VEGF-PET imaging is a noninvasive biomarker showing differential changes in the tumor during sunitinib treatment. Cancer Res. 2011;71(1):143–53.
50. Xie L, Yui J, Fujinaga M, et al. Molecular imaging of ectopic metabotropic glutamate 1 receptor in melanoma with a positron emission tomography radioprobe (18)F-FITM. Int J Cancer. 2014;135(8):1852–9.
51. Fujinaga M, Xie L, Yamasaki T, et al. Synthesis and evaluation of 4-halogeno-N-[4-[6-(isopropylamino)pyrimidin-4-yl]-1,3-thiazol-2-yl]-N-[11C]methylbenzamide for imaging of metabotropic glutamate 1 receptor in melanoma. J Med Chem. 2015;58(3):1513–23.